Development 139, 537-546 (2012) doi:10.1242/dev.073932

αE-catenin regulates cell-cell adhesion and membrane blebbing during zebrafish epiboly

Antonino Schepis[1,*], Diane Sepich[2] and W. James Nelson[1,3]

SUMMARY

αE-catenin is an actin-binding protein associated with the E-cadherin-based adherens junction that regulates cell-cell adhesion. Recent studies identified additional E-cadherin-independent roles of αE-catenin in regulating plasma membrane dynamics and cell migration. However, little is known about the roles of αE-catenin in these different cellular processes in vivo during early vertebrate development. Here, we examined the functions of αE-catenin in cell-cell adhesion, cell migration and plasma membrane dynamics during morphogenetic processes that drive epiboly in early *Danio rerio* (zebrafish) development. We show that depletion of αE-catenin caused a defect in radial intercalation that was associated with decreased cell-cell adhesion, in a similar manner to E-cadherin depletion. Depletion of αE-catenin also caused deep cells to have protracted plasma membrane blebbing, and a defect in plasma membrane recruitment of ERM proteins that are involved in controlling membrane-to-cortex attachment and membrane blebbing. Significantly, depletion of both E-cadherin and αE-catenin suppressed plasma membrane blebbing. We suggest that during radial intercalation the activities of E-cadherin and αE-catenin in the maintenance of membrane-to-cortex attachment are balanced, resulting in stabilization of cell-cell adhesion and suppression of membrane blebbing, thereby enabling proper radial intercalation.

KEY WORDS: Blebbing, Cell-cell adhesion, Cell migration, Epiboly, Gastrulation, Zebrafish

INTRODUCTION

The adherens junction (AJ) comprises protein complexes involved in cell-cell adhesion and collective cell migration in embryonic development (Halbleib and Nelson, 2006). Cell-cell adhesion at the AJ is mediated by classical cadherins, such as E-cadherin, via trans interactions between their extracellular domains on opposing cells (Stemmler, 2008). The cytoplasmic domain of classical cadherins binds β-catenin and p120-catenin (Shapiro and Weis, 2009), and β-catenin in turn binds the actin-binding protein α-catenin that connects the AJ with the actin cytoskeleton (Benjamin and Nelson, 2008). α-Catenin might have additional roles in cell polarity, signal transduction and as a tension transducer (Gladden et al., 2010; Yonemura et al., 2010; Schlegelmilch et al., 2011).

Early models proposed that vertebrate α-catenin provides a static bridge between the AJ and the actin cytoskeleton (Rimm et al., 1995). However, recent studies have caused a re-evaluation of α-catenin regulation and function. In vitro biochemical studies revealed that αE-catenin exists as either a monomer that binds strongly to β-catenin but weakly to F-actin, or a homodimer that binds strongly to F-actin but not to β-catenin, and the homodimer exist as a cytoplasmic pool (Drees et al., 2005; Yamada et al., 2005; Benjamin et al., 2010). These studies raised the possibility that αE-catenin regulates F-actin independently of the E-cadherin cell-cell adhesion complex. In fact, selective depletion of the αE-catenin cytoplasmic pool increased lamellipodial activity and the rate of cell migration without affecting cell-cell adhesion (Benjamin et al., 2010; Borghi et al., 2010). Thus, αE-catenin appears to play roles in maintaining cell-cell adhesion and suppressing membrane dynamics associated with cell migration.

Gastrulation is a crucial stage of animal development that depends on morphogenetic processes (including epiboly) that involve cell migration, cell sorting and tissue remodeling while maintaining cell-cell adhesion (Solnica-Krezel, 2005). Epiboly is defined as the spreading and thinning of one tissue over another (Lepage and Bruce, 2010). In *Danio rerio* (zebrafish) gastrulation, two tissues undergo epiboly to spread over and enclose the yolk cell: the external-most cell layer, which is termed the enveloping layer (EVL), and the deep cells, which become the embryo proper (Lepage and Bruce, 2010). EVL epiboly may be driven by the changing morphology of the yolk syncytial layer (YSL) (Koppen et al., 2006), a cytosolic, yolk-free region of the yolk cell found immediately under the deep cells that also spreads during epiboly (Carvalho and Heisenberg, 2010). The leading edge of the EVL and the YSL are connected by tight junctions, and depletion of the tight junction protein claudin E impairs EVL epiboly (Siddiqui et al., 2010). The YSL might provide a pulling force on the EVL margin through an actin ring just below the EVL margin (Koppen et al., 2006). A major contributor to deep cell epiboly is radial intercalation, in which deeper cells intercalate between and displace more superficial cells causing the presumptive ectoderm to become thinner and spread over the yolk (Kane et al., 2005; Lepage and Bruce, 2010).

E-cadherin (Cdh1 – Zebrafish Information Network) plays a crucial role during zebrafish gastrulation. Loss of E-cadherin expression due to mutation or depletion by morpholino arrests deep cell epiboly at mid-gastrulation (Babb and Marrs, 2004; Kane et al., 2005; Shimizu et al., 2005). The delay in epiboly in E-cadherin mutants and morphants appears to be due to defective radial intercalation. Mutant or morphant deep cells fail to stably integrate into the superficial layer and drop back to the lower layer, thereby

[1]Department of Biology, Stanford University, Stanford, CA 94304, USA. [2]Department of Developmental Biology, Washington University School of Medicine, St. Louis, MO 63110, USA. [3]Department of Molecular and Cellular Physiology, Stanford University, Stanford, CA 94304, USA.

*Author for correspondence (antonino.schepis@kcl.ac.uk)

Accepted 23 November 2011

slowing or blocking epiboly (Kane et al., 2005; Slanchev et al., 2009). By contrast, E-cadherin is not required for EVL epiboly (Shimizu et al., 2005; Koppen et al., 2006; Lin et al., 2009).

Few studies have examined the role of αE-catenin in cellular dynamics during early vertebrate development. In *Xenopus*, depletion of αE-catenin causes a delay in gastrulation (Kofron et al., 1997), and genetic deletion of αE-catenin (Ctnna1 – Mouse Genome Informatics) in mice is lethal in the pre-implantation stage (Torres et al., 1997). Here, we analyzed the role of αE-catenin at the single cell level during coordinated cell movements in vertebrate epiboly, and show that αE-catenin plays roles in cell-cell adhesion, membrane dynamics and cell migration.

MATERIALS AND METHODS

Zebrafish maintenance

Zebrafish wild-type embryos were raised at 28.5°C and staged as described (Kimmel et al., 1995). Wild-type strains TL and WIK were used.

Antibodies and reagents

Primary antibodies used were: α-catenin (for western blotting, BD; for immunostaining, Sigma), pan-cadherin, β-catenin and tubulin (Sigma); pERM and pMLC (Cell Signaling); HA-tag (Covance); zebrafish E-cadherin (Babb and Marrs, 2004). Rhodamine Phalloidin was obtained from Invitrogen, blebbistatin from Sigma. Antisense morpholinos (Gene-Tools) used were: *ctnna* morpholino 1 (targeting 5′UTR), CAAAATGGAGGGATGAGACTTTTAC; *ctnna* mismatch morpholino 1, CAAATTCGACGGATGACAGTTTTAC; *ctnna* morpholino 2, TAATGCTCGTCATGTTCCAAATTGC; *cdh1* morpholino, ATCCCACAGTTGTTACACAAGCCAT (Babb and Marrs, 2004); *ezr* morpholino, CGCGAACATTTACTGGTTTAGGCAT (Link et al., 2006). Capped mRNA was synthesized using mMessage-Machine (Ambion).

Cloning zebrafish *ctnna* and mouse *gfp-Ctnna1*

Zebrafish *ctnna* c-DNA was obtained from Open Biosystems (Image ID 2639279) and subcloned into pCS2^{+}. The HA tag was introduced through the 3′ primer sequence. Mouse *gfp-mctnna* (Benjamin et al., 2010) was subcloned in pCS2^{+}.

RNA and antisense morpholino injection

Capped mRNA and antisense morpholino were injected at the 1- to 2-cell stage at the following doses: membrane localized GFP (Wallingford et al., 2000), 100 pg; *ctnnaha*, 200 pg; *gfp-mctnna*, 200 pg; *ctnna* morpholino1, 4 ng (high dose) and 0.8 ng (low dose); *ctnna* mismatch morpholino1, 5 ng; *ctnna* morpholino2, 10 ng; *cdh1* morpholino, 8 ng; *ezr* morpholino, 8 ng (high dose) and 1 ng (low dose).

Whole-mount immunostaining

Embryos were fixed in 4% paraformaldehyde in PBS. Whole-mount immunohistochemistry was performed as described previously (Koppen et al., 2006).

Microscopy and imaging analysis

Live embryos were mounted in 2% methylcellulose in 0.3× Danieau's buffer at 28.5°C (Saude et al., 2000). Embryos at segmentation stages were imaged with an Axiovert microscope (Carl Zeiss). Differential interference contrast (DIC) and confocal images were taken using an LSM 510 (Carl Zeiss).

Image analysis was performed using ImageJ software (http://rsbweb.nih.gov/ij/). Time-lapse images were recorded for 20 minutes at ~1 minute intervals, or for 5 minutes at 4 second intervals. The imaging focal plane was set at 6-8 μm from the basal membrane of EVL at the animal pole. The 20 minute time-lapse recordings used embryos at 50-60% epiboly. The 5 minute time-lapse recordings used embryos at 50% epiboly. For the blebbistatin experiments, embryos were incubated in 50 μM blebbistatin or DMSO for 30 minutes.

Radial intercalation and reverse radial intercalation rate represent the percentage of cell undergoing radial intercalation (RI) or reverse radial intercalation (revRI) of the total population of cells in the field of view at the end of the recording period (20 minutes).

Staging by 'percent epiboly' was calculated by measuring the distance from animal pole to the EVL or deep cell margins, and dividing by the animal-vegetal axis length. Three independent experiments were performed; n=25 embryos.

Length-to-width ratio of the deep cells at the margin was measured as previously described (Koppen et al., 2006). Three independent experiments were performed; n=40 cells (eight embryos).

The fluorescence intensity (FI) determination for phosphorylated myosin light chain (pMLC) staining was performed as previously described (Kitt and Nelson, 2011). Three independent experiments were performed; n=300 cell contacts (15 embryos). The control was normalized to one.

Transplantation experiments

Wild-type embryos were injected with membrane-localized GFP mRNA with or without *ctnna* morpholino 1. Labeled cells were transplanted at the blastula stage into control or morphant hosts.

Whole-mount in situ hybridization (ISH)

Embryos were collected at dome stage and fixed with 4% paraformaldehyde overnight at 4°C. Whole-mount ISH was performed as described (Thisse and Thisse, 1998). Probes used were: *Keratin4* (Thisse et al., 2001), *no tail* (Schulte-Merker et al., 1992) and *pax2.1* (Krauss et al., 1992).

Cell aggregation assay

Dome stage embryos were dispersed using trypsin/EDTA. The cells were plate at a concentration of 5000 cells/ml and incubated overnight at 28.5°C overnight with or without EGTA (5 mM).

Western blotting

Embryo homogenates were lysed with 4×lysis buffer (62.5 mM Tris-HCl pH 6.8, 10% glycerol, 2% SDS, 0.5% β-mercaptoethanol, 0.01% Bromophenol Blue) and heated at 100°C for 5 minutes. Extracts were resolved in a 6% polyacrylamide gel and transferred to a PVDF membrane using the Criterion System (Bio-Rad).

Statistical analysis

Statistical analyses were performed using an unpaired t-test with unequal variance using Excel (Microsoft) and Prism (Graph Pad).

RESULTS

αE-catenin is required for early zebrafish development

αE-catenin (Ctnna – Zebrafish Information Network) is ubiquitously expressed during gastrulation and early zebrafish development (Dong et al., 2009; Slanchev et al., 2009). This was confirmed by immunofluorescence microscopy of whole-mount embryos and western blotting of embryo extracts with antibodies specific for αE-catenin (supplementary material Fig. S1A-D; see also Fig. 1D and Fig. 2D).

To investigate the role of αE-catenin in early zebrafish development, we blocked *ctnna* mRNA translation by injecting two different translation blocking morpholinos (mo): *ctnna* mo1 targeted the 5′UTR of *ctnna* mRNA, and *ctnna* mo2 targeted a sequence that overlaps with 5′UTR and the open reading frame (ORF). Embryos injected with 4 ng of *ctnna* mo1, but not uninjected control embryos, had defects in morphology at the end of gastrulation (95.2±4.8%; Fig. 1A-C,I). Embryos injected with 10 ng of *ctnna* mo2 also displayed the same morphological defects as *ctnna* mo1, but with weaker penetrance (79.9±4.4%; Fig. 1I). Some *ctnna* morphants did not close the blastopore over the yolk (Fig. 1C, arrow).

The specificity of the epibolic defect caused by *ctnna* mo1 was shown by three types of experiments. First, injection of a mismatched mo1 (mm-mo1; 5ng) did not cause epibolic defects (1.5±1.1%; Fig. 1I). Second, αE-catenin was depleted by *ctnna*

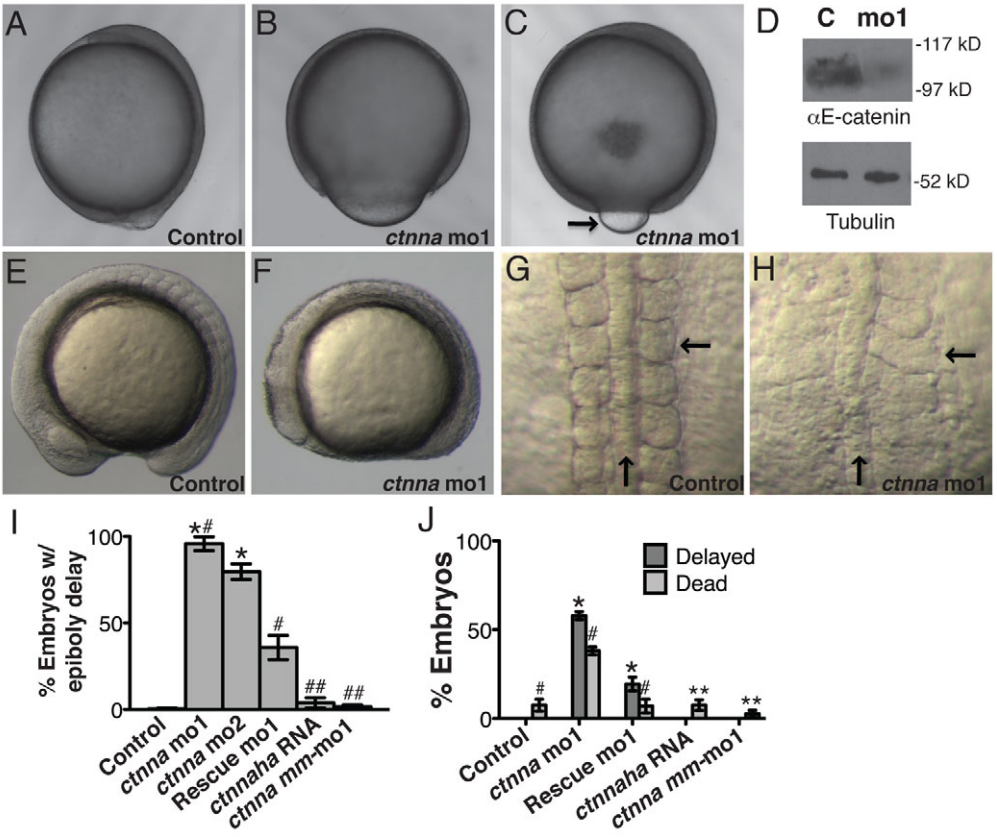

Fig. 1. *ctnna* morphants display morphological defects. (**A-C**) DIC images of live zebrafish embryos at the end of gastrulation. Arrow indicates yolk bulge. (**D**) Western blot of αE-catenin and tubulin in whole-embryo extracts at the same stages as those shown in A-C. (**E**,**F**) Lateral view images of live embryos at the mid-segmentation stage. (**G**,**H**) Images of live embryos, dorsal view. Horizontal arrow indicates somite, vertical arrow indicates notochord. (**I**) Percentage of embryos exhibiting epiboly delay at the end of gastrulation, as shown in B,C. Three independent experiments with $n>70$: $^{*}P<10^{-6}$ versus control, $^{\#}P<10^{-5}$ versus rescue. ##, not significantly different from control by Student's *t*-test. (**J**) Fraction of embryos dead or delayed by mid-segmentation, as shown in E,F. Three independent experiments, $n>70$ embryos. $^{*}P<10^{-6}$, # control or rescue vs morphant $P<10^{-5}$. **, not significant. Error bars indicate s.d.

mo1 as shown by western blotting of whole embryo extracts at 90% epiboly (Fig. 1D). Third, the defects caused by the *ctnna* mo1 were rescued by co-injecting the *ctnna* mo1 with a synthetic mRNA for αE-catenin tagged with HA (*ctnnaha*), which did not bind the mo1; only 35.9±7% of rescued mo1 embryos had defects in morphology at the end of gastrulation (Fig. 1I). Note that αE-catenin-HA was expressed and localized at the plasma membrane and cytoplasm of deep cells (Fig. 2G) and EVL (A.S., unpublished results). Injection of up to 200 pg of *ctnnaha* mRNA alone did not cause any apparent developmental defects (Fig. 1I).

To understand whether the delay in epiboly in the *ctnna* morphant was due to a morphological or developmental defect, we performed in situ hybridization (ISH) for *no tail* and *pax2.1* (*pax2a* – Zebrafish Information Network) in embryos fixed at 80% epiboly (supplementary material Fig. S1E,F). The ISH for *no tail* revealed a pattern that was typical for a delay in epiboly (Babb and Marrs, 2004). By contrast, *pax2.1* expression was absent from the *ctnna* morphant at a stage at which it was already present in the control; note that *pax2.1* expression appeared after 90% epiboly in the *ctnna* morphant (not shown). The delay in *pax2.1* expression indicates that depletion of αE-catenin caused a developmental delay.

At later stages of embryogenesis (mid-segmentation), 57.9±2.9% of embryos injected with *ctnna* mo1 had a strong developmental delay, and those that reached the mid-segmentation stage had an abnormal morphology (Fig. 1E-H,J). Furthermore, 38±2.9% of the embryos died by mid-segmentation. Rescue of *ctnna* mo1 reduced the percentage of delayed embryos to 19.4±3.4% and the percentage of dead embryos to 7±3.4% (Fig. 1J). All of the *ctnna* morphants displayed defects in notochord and somite morphology (Fig. 1G,H). Injection of the *ctnna* mm-mo1 did not cause any defects at this stage (2±1.5% dead embryos, Fig. 1J), whereas injection of *ctnna* mo2 caused complete lethality (A.S., unpublished results). These defects in later stages of embryogenesis were not pursued further. Instead, we focused on defects in epiboly to study αE-catenin functions in cell-cell adhesion, membrane dynamics and cell migration. For the rest of this study, we did not use the *ctnna* mo2 owing to the weak penetrance in the epibolic defect; from this point, we refer to *ctnna* mo1 and mm-mo1 as *ctnna* mo and mm-mo, respectively.

αE-catenin depletion causes a delay in epiboly

To investigate the delay in gastrulation caused by αE-catenin depletion, we measured the extent of epiboly at mid-gastrulation. Uninjected embryos or embryos injected with *ctnna* mo, *ctnna* mo + *ctnnaha* mRNA (rescue), or *ctnnaha* mRNA were fixed at 80% epiboly, as defined by the control uninjected cohort. Embryos were stained with a β-catenin antibody to mark the plasma membrane for analysis of embryos by confocal microscopy (Fig. 2A-C); percentage epiboly was defined as the distance between the animal pole and the EVL or deep cell margins (Fig. 2A-C, arrows). Compared with the control, *ctnna* morphants were delayed in the migration of both the EVL margin (80.8±2.02% epiboly; control, 88.9±0.8% epiboly) and deep cell margin (71.4±2.16% epiboly; control, 83.7±1.7% epiboly) (Fig. 2A,B,H). Rescue embryos were not delayed (Fig. 2C,H), nor were embryos injected with *ctnnaha* mRNA (Fig. 2H).

We analyzed the levels of αE-catenin at 50% epiboly by immunostaining whole-mount embryos in order to confirm that it had been depleted in the deep cells. *Ctnna* morphant deep cells had significantly reduced levels of αE-catenin at the plasma membrane

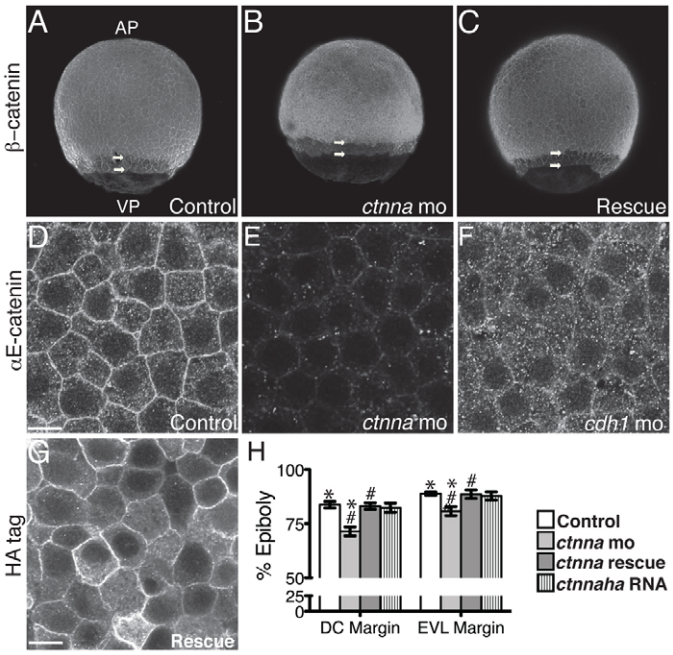

Fig. 2. ctnna morphants are delayed in epiboly.
(**A-C**) Immunofluorescence images of fixed zebrafish embryos stained for β-catenin. AP, animal pole; VP, vegetal pole. Upper arrow indicates deep cell margin, lower arrow indicates EVL margin. (**D-F**) Confocal fluorescence images of Ctnna antibody staining of the most external epiblast layer at the animal pole of embryos at 50% epiboly. Scale bar: 10 μm. (**G**) Rescue embryos stained for the HA tag; same view as D-F. Scale bar: 10 μm. (**H**) Percentage of epiboly of the deep cell (DC) and EVL margins. Three independent experiments, *n*=25 embryos. **P*<0.006, #*P*<0.001. Error bars indicate s.d.

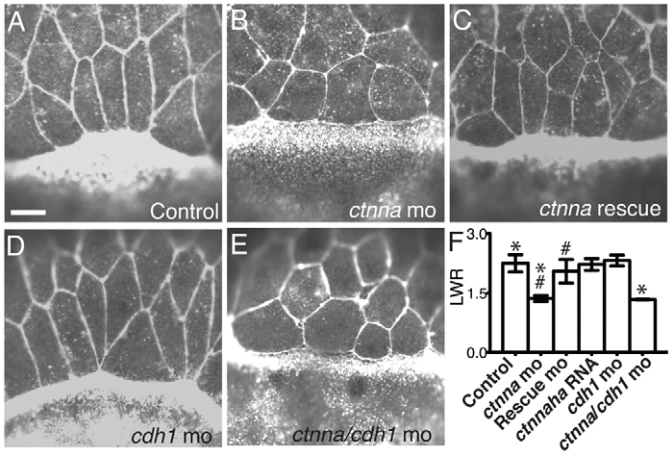

Fig. 3. αE-catenin depletion causes defects in EVL cell morphology. (**A-E**) Confocal images of cells at EVL margin at 80% epiboly stained for F-actin with rhodamine phalloidin. Scale bar: 10 μm. (**F**) Quantification of length-width ratio (LWR) of cells at the EVL margin. Three independent experiments, *n*=40 cells from eight embryos. **P*<0.002; #*P*<0.003. Error bars indicate s.d.

and in the cytoplasm compared with control (Fig. 2D,E). Note that localization of αE-catenin at the plasma membrane and cell-cell contacts was dependent on expression of E-cadherin (Fig. 2F). αE-catenin-HA was expressed and localized at the plasma membrane (Fig. 2G).

Next, we examined the morphology of cells at the EVL margin at 80% epiboly using F-actin staining. Control EVL cells had an elongated shape, which is typical of this stage (Fig. 3A). Elongation of EVL cells at the margin coincided with movement of the EVL margin toward the vegetal pole (Koppen et al., 2006). By contrast, *ctnna* morphant cells did not have this elongated morphology (Fig. 3B). This difference in morphology was shown quantitatively by measuring the length-width ratio (LWR) of EVL margin cells in control (LWR 2.25±0.22) and *ctnna* morphants (LWR 1.36±0.08) (Fig. 3F). The morphology of the cells at the EVL margin was rescued by co-injection of *ctnna* mo and *ctnnaha* mRNA (LWR 2.05±0.3) (Fig. 3C,F). Injection of *ctnnaha* mRNA alone did not cause defects in cell morphology at the EVL margin (LWR 2.22±0.18; Fig. 3F).

As αE-catenin forms a complex with E-cadherin, we compared the morphology of *ctnna* morphants with *cdh1* morphants (8 ng *cdh1* mo). We found that morphological defects in cells in the EVL margin were specific to *ctnna* morphants (LWR 1.36±0.08), and not to *cdh1* morphants (LWR 2.32±0.14) (Fig. 3D,F), as previously shown (Koppen et al., 2006; Lin et al., 2009). Moreover, co-injection of *cdh1* mo and *ctnna* mo (8 ng and 4 ng, respectively) resulted in a similar morphology to the embryos injected with *ctnna* mo only (LWR 1.33±0.01) (Fig. 3E,F).

It has been reported that defects in EVL differentiation can induce defects in epiboly (Fukazawa et al., 2010). In order to rule out the possibility that the defect in EVL morphology and the delay in epiboly were caused by a defect in EVL differentiation, we performed ISH for *keratin4* (*krt4*) mRNA at the dome stage (supplementary material Fig. S2). The *ctnna*, *cdh1* and *ctnna-cdh1* morphant embryos displayed normal *krt4* expression compared with the control, indicating that the EVL had differentiated normally in these embryos.

These results indicate that the failure of EVL margin cells to acquire an elongated morphology in *ctnna* morphants correlates with the delay in the EVL epiboly (Fig. 2B). This phenotype was not caused by E-cadherin depletion and was not rescued by co-depletion of E-cadherin and αE-catenin. Thus, αE-catenin appears to be necessary for cells at the EVL margin to acquire an elongated morphology, but E-cadherin is dispensable.

αE-catenin depletion causes a defect in radial intercalation

To investigate the nature of the deep cell margin delay (Fig. 2B,H), we used time-lapse microscopy to examine the behavior of individual deep cells (DCs) at the animal pole at 50-60% epiboly in embryos injected with mRNA for membrane-bound GFP (mbGFP). Time-lapse microscopy of control DCs undergoing radial intercalation (RI) showed that DCs appeared from a deeper layer, intercalated between other cells and were retained in the outer epiblast layer (Fig. 4A; supplementary material Movie 1). DCs in *ctnna* morphants (4 ng mo) also appeared in the superficial epiblast layer, similar to control DCs (Fig. 4B). Strikingly, however, some of the DCs in *ctnna* morphants moved back into the deeper layers (Fig. 4B; supplementary material Movie 2) in a process termed reverse radial intercalation (revRI) that was never observed in control embryos (Fig. 4A; supplementary material Movie 1).

We also analyzed the behavior of DCs in *cdh1* morphants; depletion of E-cadherin was confirmed by immunostaining using an E-cadherin-specific antibody or a pan-cadherin antibody (supplementary material Fig. S3A-D), indicating that E-cadherin is

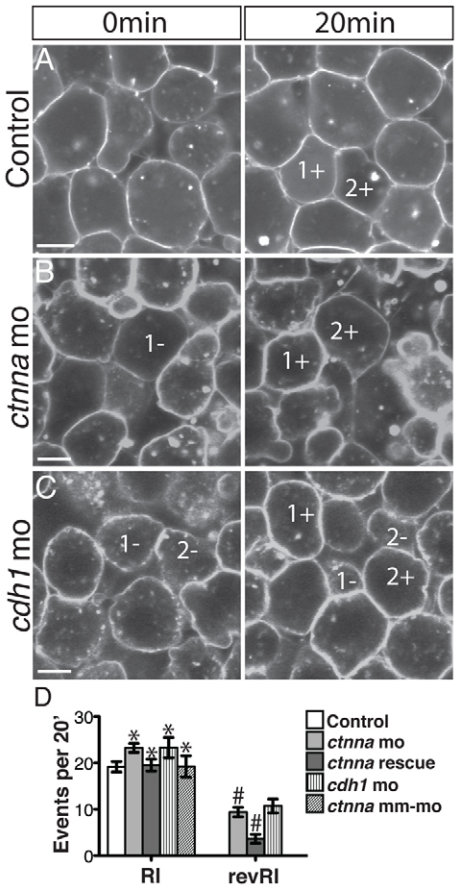

Fig. 4. αE-catenin and E-cadherin depletion causes defects in radial intercalation (RI). (**A-C**) Confocal images from time-lapse movies at the most external epiblast layer of the animal pole at 50% epiboly. Membranes are labeled with mbGFP. Positive numbers indicate cells appearing in the focal plane (undergoing RI). Negative numbers indicate cells migrating back into the in lower epiblast layer (undergoing revRI). Scale bars: 8 μm. (**D**) Quantification of RI rate and revRI. *n*=9 embryos. $^{\#}P<0.0005$. Asterisk indicates not significant. Error bars indicate s.e.m.

the predominant, if not the only, classical cadherin expressed in the most external layer of DCs at the animal pole at 50% epiboly. In *cdh1* morphants, DCs intercalated into the superficial epiblast layer (Fig. 4C; supplementary material Movie 3). Similar to *ctnna* morphants, however, some of the *cdh1* morphant DCs underwent revRI (Fig. 4C; supplementary material Movie 3). These observations confirm results of previous studies of *cdh1* mutants and morphants (Kane et al., 2005; Slanchev et al., 2009).

We measured the rates of RI and revRI, defined as the percentage of cells that intercalated into or left the external epiblast layer, respectively, during 20-minute time-lapse movies for nine embryos (Fig. 4D). The RI rate was similar in the control (19.17±1.12), *cdh1* morphant (23.19±2.3) and *ctnna* morphant (23.2±1) (Fig. 4D). We did not observe any revRI events in control embryos (rate 0), but the revRI rate was 10.7±1.5 in *cdh1* morphants and 9.3±1 in *ctnna* morphants (Fig. 4D). The revRI defect in the *ctnna* morphant was partially rescued by injection of a synthetic mRNA encoding a GFP-tagged version of mouse αE-catenin (*gfp-mctnna*) (Fig. 4D; for expression and correct cell membrane localization of GFP-αE-catenin see supplementary material Movie 9). Injection of the mismatched *ctnna* mm-mo did not alter the rate of RI (19.24±2.22; Fig. 4D) and, similar to the control embryos, did not cause any revRI events (rate 0). Finally, the revRI caused by αE-catenin depletion was cell autonomous (7/42 cells for 5 min time lapses; supplementary material Movie 4). These results indicate, as shown previously for the *cdh1* mutant/morphant (Kane et al., 2005; Slanchev et al., 2009), that the delay in DC margin epiboly was due to cells that were unable to remain in the most external epiblast layer and moved back into the deeper layers.

We explored the possibility that the revRI phenotype was caused by defects in cell-cell adhesion by performing an ex vivo cell-cell aggregation assay. Embryos were dissociated using trypsin and the cells were allowed to re-aggregate overnight. Cells from control embryos formed large cell aggregates (supplementary material Fig. S4A). Incubation of wild-type cells with 5 mM EGTA, which chelates Ca^{2+} and inhibits Ca^{2+}-dependent cadherin-mediated cell-cell adhesion, completely inhibited cell aggregation (supplementary material Fig. S4B). Depletion of E-cadherin or αE-catenin also inhibited cell-cell adhesion (supplementary material Fig. S4C,D). This result supports the hypothesis that the revRI phenotype of DCs depleted of αE-catenin is due to reduced cell-cell adhesion.

αE-catenin depletion induces increased plasma membrane blebbing

Time-lapse movies of *ctnna* morphant DCs at 50% epiboly revealed dynamic plasma membrane activity that was not observed in controls (supplementary material Movies 5, 6). To investigate the nature of this membrane activity, we took time-lapse movies at a faster interval rate (4 second intervals for 5 minutes) in the most external DCs layer at the animal pole. Time-lapse images revealed that *ctnna* morphant DCs had plasma membrane activity that resembled blebbing (Fig. 5B, arrows indicate membrane blebs; supplementary material Movie 8) (Charras et al., 2006). These cells displayed up to eight bleb-like protrusions during the time-lapse recording, with an average number of 2.44±0.17 bleb-like protrusions per cell per 5 minutes (Fig. 5D,E). By contrast, >80% of both control and *cdh1* morphant cells had no bleb-like activity, and the remainder had fewer than three bleb-like activities over the same period (Fig. 5A,C,D; supplementary material Movies 7, 10); overall, the average bleb-like activity of both control and *cdh1* morphant cells was ~0.2 per cell (Fig. 5E). Co-injection of *gfp-mctnna* mRNA with *ctnna* mo reduced the number of bleb-like protrusions to an average similar to that observed in control embryos (0.49±0.11) (Fig. 5D,E; supplementary material Movie 9), whereas injection of *gfp-mctnna* mRNA did not induce blebbing (Fig. 5D,E). Injection of the mismatched *ctnna* mm-mo did not trigger blebbing of DCs, similar to control cells (0.12±0.032 blebs per cell; Fig. 5D,E).

To address how αE-catenin regulates plasma membrane blebbing, we tested whether αE-catenin expression was required in the blebbing DCs and/or in the surrounding DCs. Transplantation experiments were performed in which DCs from *ctnna* morphants were transferred into control embryos and vice versa. Control DCs transplanted into *ctnna* morphant embryos did not display protracted plasma membrane blebbing (23/23 cells in ten embryos) (Fig. 6A; supplementary material Movie 11). By contrast, *ctnna* morphant DCs transplanted into a control cell background displayed protracted plasma membrane blebbing (22/42 cells in ten embryos Fig. 6B; supplementary material Movie 12) similar to that of DCs in the *ctnna* morphant from which they were transplanted. Thus, plasma membrane blebbing of *ctnna* morphant DCs was cell

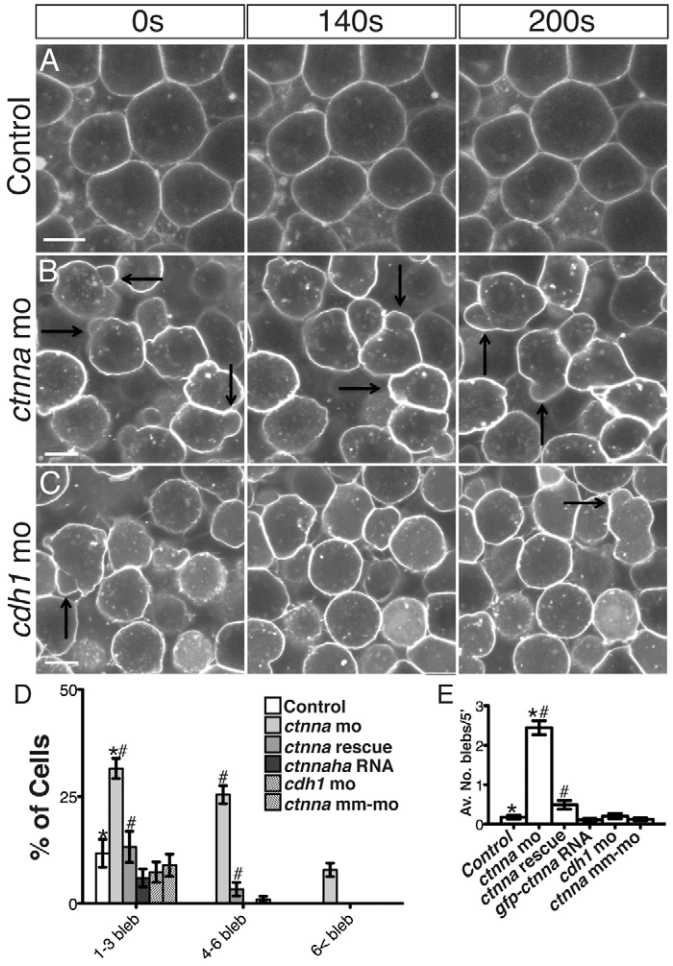

Fig. 5. αE-catenin depletion triggers protracted bleb-like protrusions. (**A-C**) Selected confocal images from time-lapse movies at the most external epiblast layer of the animal pole at 50% epiboly. Membranes are labeled with mbGFP. Arrows indicate membrane blebs. Scale bars: 8 μm. (**D**) Percentage of cells exhibiting bleb-like protrusions over 5 minutes. n=12 embryos. $^{\#}P<10^{-5}$ control versus rescue, $^{*}P<10^{-5}$ control versus morphant. Error bars indicate s.e.m. (**E**) Average number of blebs per cell over 5 minutes. n=12 embryos. $^{\#}P<10^{-8}$ control versus rescue, $^{*}P<10^{-8}$ control versus morphant. Error bars indicate s.e.m.

autonomous, and increased plasma membrane blebbing in surrounding *ctnna* morphant DCs did not provoke blebbing in control DCs.

Myosin II activity is required for plasma membrane blebbing (Blaser et al., 2006), and we tested whether myosin II was also involved in blebbing induced in *ctnna* morphants. Embryos were incubated with vector (DMSO) or blebbistatin, a well-characterized inhibitor of myosin II (Kovacs et al., 2004); note that embryos displaying multinucleated cells were not analyzed further owing to defects in cytokinesis and cell division. Blebbistatin inhibited plasma membrane blebbing in *ctnna* morphants, indicating the involvement of myosin II in this process (Fig. 6C-F, arrows indicate blebbing; supplementary material Movies 13-16).

The blebbing caused by αE-catenin depletion is E-cadherin dependent

Unlike *ctnna* morphant DCs, *cdh1* morphant DCs did not exhibit increased plasma membrane blebbing. Therefore, we investigated further the relationship between αE-catenin and E-cadherin in regulating plasma membrane blebbing. One possibility that could explain the difference in phenotype is that myosin II is activated in *ctnna* morphant DCs but not in *cdh1* morphant DCs. To explore this possibility, we performed immunostaining of whole-mount embryos at 50% epiboly using an antibody that recognized the phosphorylated form of myosin light chain (pMLC); phosphorylation of MLC is correlated with myosin II activation (Amano et al., 1996). We took confocal images of the external epiblast layer at the animal pole (Fig. 7A-C). Quantification of the fluorescence intensity (FI) of pMLC staining at cell-cell contacts revealed that pMLC is enriched equally at cell-cell contacts in both *cdh1* (FI: 1.49±0.22) and *ctnna* morphants (FI: 1.44±0.14) compared with the control FI value normalized to 1 (Fig. 7D). These results indicate that the difference in blebbing phenotype between the two morphants is not dependent on differences in myosin II activity.

Another possibility is that E-cadherin-mediated cell-cell adhesion triggers or initiates plasma membrane blebbing by contacting αE-catenin-depleted cells. To address this possibility, we performed another transplantation experiment in which *ctnna* morphant DCs were transferred into a *cdh1* morphant host. The *ctnna* morphant DCs did not show plasma membrane blebbing when they were surrounded by *cdh1* morphant DCs (34/34 cells, nine embryos; Fig. 8A; supplementary material Movie 17), in contrast to *ctnna* morphants DCs transferred into control embryos (Fig. 6A; supplementary material Movie 12). We also performed a co-depletion of E-cadherin and αE-catenin. Significantly, these morphants had very little plasma membrane blebbing (0.016±0.07 blebs for cell; Fig. 8B-D; supplementary material Movie 18), similar to *cdh1* morphants and controls embryos (Fig. 5; supplementary material Movies 7, 10), but unlike the *ctnna* morphants (2.44±0.17 blebs for cell; Fig. 5; supplementary material Movie 8). Taken together, these results indicate that plasma membrane blebbing in the *ctnna* morphant DCs is dependent on E-cadherin-mediated cell-cell contacts.

E-cadherin depletion suppresses blebbing caused by ezrin depletion

Next, we investigated the possibility that E-cadherin could function with other proteins involved in plasma membrane blebbing, such as ezrin (Ezr). Ezrin is an ERM-domain protein that regulates cell cortex stability and cell adhesion and plays important roles in blebbing dynamics (Charras and Paluch, 2008; Arpin et al., 2011); depletion of ezrin increases blebbing in zebrafish mesoderm cells (Diz-Munoz et al., 2010). We first confirmed that ezrin depletion increased blebbing of epiblast DCs. Indeed, DCs in *ezr* morphants (8 ng mo, high dose) had extensive plasma membrane blebbing (Fig. 9A,B; supplementary material Movie 19), similar to *ctnna* morphant DCs (Fig. 5B; supplementary material Movie 8).

We next investigated whether ezrin and αE-catenin synergize to suppress plasma membrane blebbing, by co-injecting embryos with low concentrations of both *ezr* and *ctnna* mo. Note that DCs in embryos injected with a low concentration of either *ctnna* mo (0.8 ng, low dose) or *ezr* mo (1 ng, low dose) did not have increased plasma membrane blebbing (Fig. 9A,B; supplementary material Movies 20, 21). However, co-injection of these low concentrations of *ezr* and *ctnna* mo resulted in increased plasma membrane blebbing (Fig. 9A,B; supplementary material Movie 22). By contrast, co-injection of a high concentration of *cdh1* mo (8 ng) and *ezr* mo (8 ng) caused a reduction in membrane blebbing compared with embryos injected with a high concentration of *ezr* mo alone (Fig. 9A,B; supplementary material Movies 19, 23). Taken

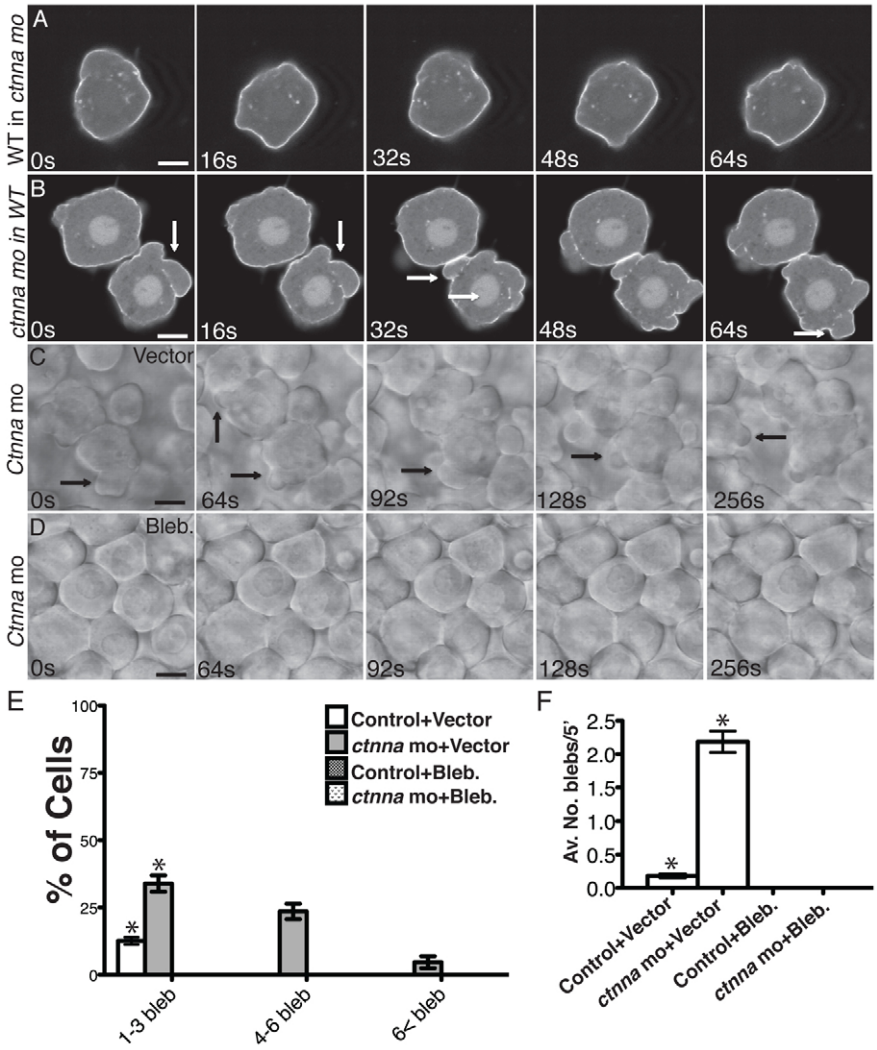

Fig. 6. Membrane blebbing triggered by αE-catenin depletion is cell autonomous and myosin II-dependent. (**A**,**B**) Selected confocal images from time-lapse movies of transplanted cells expressing mbGFP in the most external epiblast external layer of the host embryos at 50% epiboly. Arrows indicate the blebs. (A) Wild-type (WT) cell in *ctnna* morphant host embryo. (B) *ctnna* morphant cell in WT host embryo. Scale bars: 5 μm. (**C**,**D**) DIC images from time-lapse movies of untreated (DMSO) embryos or embryos treated with blebbistatin (50 μM) imaged at the most external epiblast layer at the animal pole at 50% epiboly. Scale bars: 8 μm. (**E**) Percentage of cells exhibiting bleb-like protrusions in untreated embryos or embryos treated with blebbistatin. n=12 embryos. $^{*}P<10^{-8}$, $^{\#}P<10^{-5}$. Note that no cell exhibited membrane blebbing in embryos treated with blebbistatin. Error bars indicate s.e.m. (**F**) Average number of blebs per cell untreated embryos or embryos treated with blebbistatin. n=12 embryos. $^{*}P<10^{-9}$. Note that no cell exhibited membrane blebbing in embryos treated with blebbistatin. Error bars indicate s.e.m.

together, these results indicate that blebbing in both the *ctnna* and *ezr* morphant DCs is dependent on E-cadherin-mediated cell-cell adhesion. As depletion of both ezrin and αE-catenin had an additive effect, it is likely that these proteins function in the same pathway to suppress blebbing.

ERM proteins are auto-inhibited, and this inhibition is relieved by phosphorylation, which allows binding to partners and localization at the plasma membrane (Arpin et al., 2011). We used an anti-phospho-ERM domain antibody to investigate activation and localization of ERM-domain proteins in DCs at 50% epiboly in the background of αE-catenin or E-cadherin depletion (Fig. 9C-E). Control DCs had weak phospho-ERM domain staining at the plasma membrane (Fig. 9C). By contrast, DCs in *ctnna* or *cdh1* morphants displayed strong staining at the plasma membrane, indicating activation and plasma membrane recruitment of ERM domain proteins in these mutant backgrounds (Fig. 9D,E). Note that DCs in an *ezr* morphant did not display any change in the staining intensity or subcellular localization of αE-catenin or E-cadherin (supplementary material Fig. S5); however, we cannot exclude the possibility that the lack of changes in E-cadherin and αE-catenin localization in *ezrin* morphant is due to the activity of moesin (Link et al., 2006). These results indicate that αE-catenin and E-cadherin localize to the plasma membrane independently of ezrin, and that they might be involved in regulating cycles of ERM protein activation and inactivation required for plasma membrane.

DISCUSSION

Recent biochemical studies and analysis in mammalian tissue culture cells have indicated important roles for the actin-binding protein αE-catenin in both E-cadherin-mediated cell-cell adhesion and an E-cadherin-independent role in controlling membrane dynamics and cell migration (Benjamin and Nelson, 2008; Borghi et al., 2010). E-cadherin mediated cell-cell adhesion and cell migration are regulated by the actin cytoskeleton (Harris and Tepass, 2010), and must be coordinated during complex cell movements in gastrulation (Hammerschmidt and Wedlich, 2008). Here, we investigated the role of αE-catenin in early zebrafish development during coordinated cell movements in epiboly.

The *ctnna* morphant displayed an abnormal morphology (Fig. 1C) and a strong delay in epiboly (Fig. 1B) compared with controls. As shown in Figs 2 and 3, depletion of αE-catenin affected epiboly of both the EVL and deep cell layers. The combination of defects observed in those tissues might contribute to the overall delay in epiboly and abnormal morphology shown in Fig. 1B,C. The observation that both the EVL and deep cell layers were affected and that there was a delay in onset of *pax2.1* expression (supplementary material Fig. S1E,F) indicates that, in addition to these morphological defects, there might be a developmental delay in the *ctnna* morphant. An intriguing possibility is that the delay of *pax2.1* expression could be caused

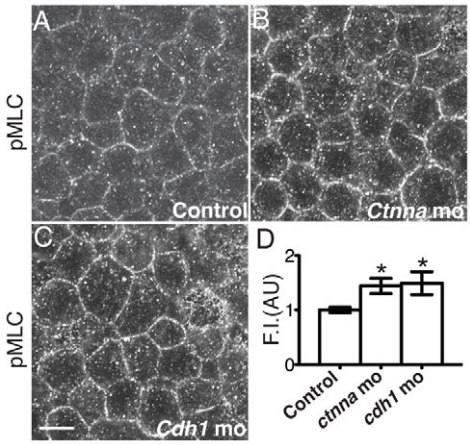

Fig. 7. *cdh1* and *ctnna* morphant DCs displayed increased phospho-MLC at cell contacts. (**A-C**) Confocal images of the epiblast most external layer at the animal pole of embryos at 50% epiboly stained for phospho-MLC. Scale bar: 10 μm. (**D**) Fluorescence intensity (FI) at cell contacts of embryos stained for pMLC. Three independent experiments, *n*=300 cell contacts (15 embryos) per experiment. **P*<10^{-3} versus the control (normalized to 1). Error bars indicate s.d.

by the defect in cell adhesion described in Fig. 4 and supplementary material Fig. S4. Additional experiments are needed to understand the possible role of αE-catenin in the YSL.

The delay in the EVL cell margin correlated with the failure of cells at the margin to elongate properly (Fig. 3). There is a correlation between the elongation of these cells and the advancing EVL margin (Koppen et al., 2006). In contrast to the *ctnna* morphants, the *cdh1* morphants did not displayed a cell elongation defect (Fig. 3), as reported by others (Shimizu et al., 2005; Koppen et al., 2006; Lin et al., 2009). Furthermore, depletion of E-cadherin did not rescue the EVL morphology defects in the background of the *ctnna* morphant. These results indicate that whereas E-cadherin is dispensable for the EVL epiboly, αE-catenin is necessary for this process. Although we cannot exclude the possibility that the function of E-cadherin is replaced by another cell-cell contact complex, such as tight junctions (Siddiqui et al., 2010), we suggest that this phenotype might reflect the role of αE-catenin in regulating the actin cytoskeleton independently of E-cadherin. This function of αE-catenin might take place in the EVL and/or in the YSL.

The delay in epiboly of the deep cell margin in the *ctnna* morphant was caused by defects related to cellular processes during RI (Figs 2, 4; supplementary material Movies 1-4). *Ctnna* morphant deep cells were capable of RI but were unable to stabilize cell-cell contacts with their neighbors in the external layer, and subsequently moved back into the deeper layer in a process that we term reverse radial intercalation (revRI) (Fig. 4; supplementary material Movies 2-4). Significantly, *cdh1* morphants had a similar phenotype to *ctnna* morphants (Fig. 3; supplementary material Movie 3), as shown previously for *cdh1* mutants (Kane et al., 2005; Slanchev et al., 2009). Using ex vivo cell aggregation assays, we also showed that depletion of αE-catenin impaired cell-cell adhesion to a similar extent as E-cadherin depletion or Ca^{2+} chelation (supplementary material Fig. S4). These results indicate that *ctnna* and *cdh1* morphant deep cells share the same defect in cell-cell adhesion and, thus, αE-catenin appears to be important in E-cadherin-mediated adhesion between deep cells and the overlying EVL (Shimizu et al., 2005; Slanchev et al., 2009). Taken together, these data highlight the importance of αE-catenin in E-cadherin-dependent cell-cell adhesion in early zebrafish development.

However, our results also identified differences in cell behavior in *ctnna* and *cdh1* morphants (Fig. 5; supplementary material Movies 5-10). *Ctnna* morphant deep cells exhibited extensive plasma membrane blebbing, which was not observed in the *cdh1* morphant or controls. Significantly, plasma membrane blebbing in *Ctnna* morphants was cell autonomous (Fig. 6; supplementary material Movies 11, 12).

Recent studies have highlighted the importance of plasma membrane blebbing in cell migration in certain cell types (Cunningham et al., 1992; Blaser et al., 2006; Fackler and

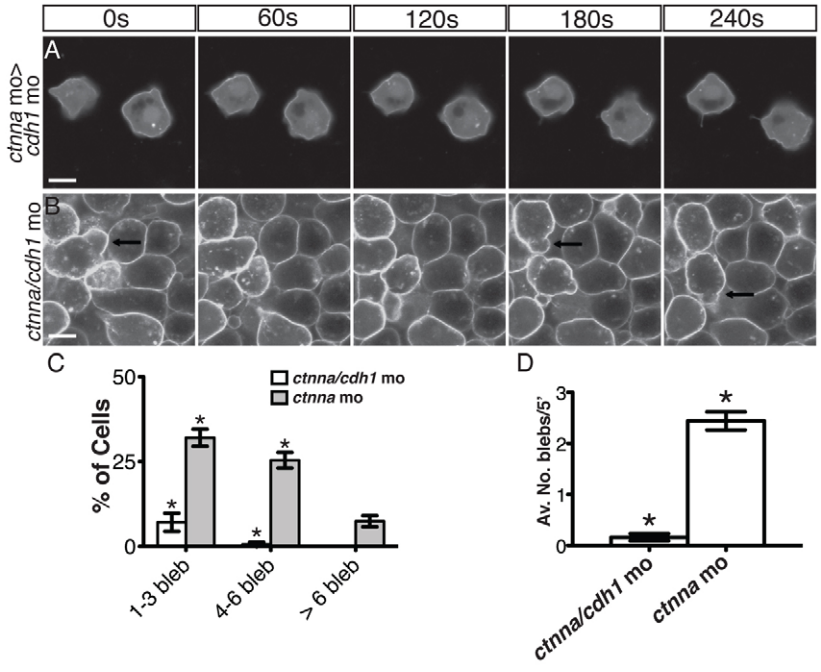

Fig. 8. Blebbing triggered by αE-catenin depletion is E-cadherin dependent. (**A**) Selected confocal images from time-lapse movies of transplanted *ctnna* morphant cells expressing mbGFP in the most external epiblast external layer of the host *cdh1* morphant embryos at 50% epiboly. Scale bar: 5 μm. (**B**) Confocal images from time-lapse movies at the most external epiblast layer of the animal pole of live embryos at 50% epiboly. Membranes are labeled with mbGFP. Arrows indicate membrane blebs. Embryos were co-injected with *cdh1* and *ctnna* mo. Scale bar: 8 μm. (**C**) Percentage of cells exhibiting bleb-like protrusions. *n*=12 embryos. **P*<10^{-5}. Error bars indicate s.e.m. (**D**) Average number of blebs per cell. *n*=12 embryos. **P*<10^{-8}. Error bars indicate s.e.m.

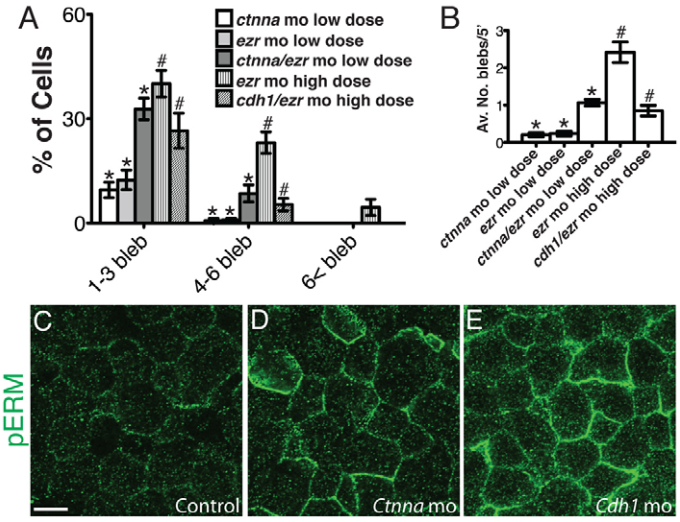

Fig. 9. αE-catenin and E-cadherin depletion influence ERM protein localization and membrane blebbing in *ezr* morphants. (**A**) Percentage of cells with bleb-like membrane protrusions. n=12 embryos. *$P<10^{-6}$ *ezr* or *ctnna* mo low dose versus *ctnna/ezr* mo low dose, #$P<10^{-6}$ *ezr* mo high dose versus *cdh1/ezr* mo high dose. (**B**) Average number of blebs per cell. n=12 embryos. *$P<10^{-6}$ *ezr* or *ctnna* mo low dose versus *ctnna/ezr* mo low dose, #$P<10^{-5}$ *ezr* mo high dose versus *cdh1/ezr* mo high dose. Error bars indicate s.e.m. (**C-E**) Confocal images of the most external epiblast layer at the animal pole of embryos at 50% epiboly stained for phospho-ERM proteins. (C) Uninjected control. (D) *ctnna* morphant. (E) *cdh1* morphant. Scale bar: ~10 μm.

Grosse,2008). Blebbing is a type of plasma membrane protrusion driven by detachment of the plasma membrane from the cell cortex and cytoplasmic hydrostatic pressure that causes the plasma membrane to transiently protrude outwards (Charras and Paluch, 2008; Tinevez et al., 2009). Plasma membrane blebbing, unlike lamellipodial formation, does not involve actin polymerization in this initial protruding phase. Once the membrane bleb is formed, ERM proteins, such as ezrin or moesin, are recruited to the plasma membrane to reconnect the membrane to the actin cytoskeleton in the cell cortex (Charras et al., 2006; Diz-Munoz et al., 2010). Finally, activation of Rho signaling and myosin II activity, and F-actin assembly cause retraction of the membrane bleb (Charras et al., 2006; Charras and Paluch, 2008; Kardash et al., 2010).

We investigated mechanisms that might trigger plasma membrane blebbing in *ctnna* morphant DCs. Immunostaining for pMLC showed that there was an enrichment of activated myosin II in both morphant DCs, compared with controls (Fig. 7). This result indicates that the lack of membrane blebbing in the *cdh1* morphant was not due to reduced activation of actomyosin contractility.

We also observed that depletion of E-cadherin or αE-catenin caused increased levels of phospho-ERM domain proteins at the plasma membrane (Fig. 9C-E). For the *ctnna* morphant, this might be in response to increased blebbing because ERM proteins are recruited to the site of blebbing in order to retract the bleb (Charras et al., 2006). However, this could not be the case in *cdh1* morphant cells that lack blebbing. Alternatively, recruitment of ERM protein to the plasma membrane might be independent of blebbing. ERM domain proteins regulate adherens junction assembly and positioning (Van Furden et al., 2004; Pilot et al., 2006; Arpin et al., 2011), and increased pERM staining in *cdh1*, and perhaps *ctnna* morphant cells, might be a response to reduced levels of functional adherens junctions.

To address the relationship between αE-catenin and E-cadherin in blebbing, we showed that the blebbing phenotype of *ctnna* morphant cells could be rescued by either transplanting *ctnna*-depleted cells into a *cdh1* morphant background, or co-depletion of αE-catenin and E-cadherin in the same cells (Fig. 8; supplementary material Movies 17, 18). Moreover, this pathway involves ERM domain proteins as suboptimal co-depletion of ezrin and αE-catenin caused blebbing, and co-depletion of ezrin and E-cadherin rescued the blebbing phenotype induced by ezrin depletion alone. Taken together with recent studies (Kardash et al., 2010; Speirs et al., 2010), our results demonstrate that plasma membrane blebbing induced by either αE-catenin or ezrin depletion is dependent on E-cadherin-mediated cell-cell engagement/adhesion.

We suggest that as deep cells in the most external layer became more adhesive (Kane et al., 2005), increased E-cadherin levels decrease the membrane-to-cortex attachment that normally opposes membrane blebbing. We posit that αE-catenin, like ezrin, counter this by stabilizing membrane-to-cortex attachment and suppressing membrane blebbing. Normally, this allows deep cells to complete radial intercalation and establish cell-cell adhesion with each other and the overlying EVL. This balance between functions of E-cadherin and αE-catenin-ezrin is disrupted by depleting αE-catenin or ezrin, which results in weaker membrane-to-cortex attachment and protracted membrane blebbing (Figs 5, 9), and is counter-balanced by co-depletion of E-cadherin (Figs 8, 9). This is the first insight into the diverse roles of αE-catenin during early stages of vertebrate development in vivo, not only in cell-cell adhesion as shown previously in *Xenopus* and mice (Kofron et al., 1997; Torres et al., 1997), but also in regulating membrane dynamics and cell migration as suggested from studies in tissue culture cells (Benjamin et al., 2010; Borghi et al., 2010).

Acknowledgements
We thank Will Talbot and Lilianna Solnica-Krezel for training and advice. We thank Dr James Marrs for the zebrafish E-cadherin antibody.

Funding
This work was supported by a grant from the National Institutes of Health (NIH) [GM35527 to W.J.N.]; and by a Marie Curie Outgoing International Fellowship (MC OIF) [PIOF-GA-2009-236027 to A.S.]. A.S. thanks Darren Gilmour and the European Molecular Biology Laboratory (EMBL) for sponsoring the MC OIF. Deposited in PMC for release after 12 months.

Competing interests statement
The authors declare no competing financial interests.

Supplementary material
Supplementary material available online at
http://dev.biologists.org/lookup/suppl/doi:10.1242/dev.073932/-/DC1

References

Amano, M., Ito, M., Kimura, K., Fukata, Y., Chihara, K., Nakano, T., Matsuura, Y. and Kaibuchi, K. (1996). Phosphorylation and activation of myosin by Rho-associated kinase (Rho-kinase). *J. Biol. Chem.* **271**, 20246-20249.
Arpin, M., Chirivino, D., Naba, A. and Zwaenepoel, I. (2011). Emerging role for ERM proteins in cell adhesion and migration. *Cell Adh. Migr.* **5**, 199-206.
Babb, S. G. and Marrs, J. A. (2004). E-cadherin regulates cell movements and tissue formation in early zebrafish embryos. *Dev. Dyn.* **230**, 263-277.
Benjamin, J. M. and Nelson, W. J. (2008). Bench to bedside and back again: molecular mechanisms of alpha-catenin function and roles in tumorigenesis. *Semin. Cancer Biol.* **18**, 53-64.
Benjamin, J. M., Kwiatkowski, A. V., Yang, C., Korobova, F., Pokutta, S., Svitkina, T., Weis, W. I. and Nelson, W. J. (2010). AlphaE-catenin regulates actin dynamics independently of cadherin-mediated cell-cell adhesion. *J. Cell Biol.* **189**, 339-352.

Blaser, H., Reichman-Fried, M., Castanon, I., Dumstrei, K., Marlow, F. L., Kawakami, K., Solnica-Krezel, L., Heisenberg, C. P. and Raz, E. (2006). Migration of zebrafish primordial germ cells: a role for myosin contraction and cytoplasmic flow. *Dev. Cell* **11**, 613-627.
Borghi, N., Lowndes, M., Maruthamuthu, V., Gardel, M. L. and Nelson, W. J. (2010). Regulation of cell motile behavior by crosstalk between cadherin- and integrin-mediated adhesions. *Proc. Natl. Acad. Sci. USA* **107**, 13324-13329.
Carvalho, L. and Heisenberg, C. P. (2010). The yolk syncytial layer in early zebrafish development. *Trends Cell Biol.* **20**, 586-592.
Charras, G. and Paluch, E. (2008). Blebs lead the way: how to migrate without lamellipodia. *Nat. Rev. Mol. Cell Biol.* **9**, 730-736.
Charras, G. T., Hu, C. K., Coughlin, M. and Mitchison, T. J. (2006). Reassembly of contractile actin cortex in cell blebs. *J. Cell Biol.* **175**, 477-490.
Cunningham, C. C., Gorlin, J. B., Kwiatkowski, D. J., Hartwig, J. H., Janmey, P. A., Byers, H. R. and Stossel, T. P. (1992). Actin-binding protein requirement for cortical stability and efficient locomotion. *Science* **255**, 325-327.
Diz-Munoz, A., Krieg, M., Bergert, M., Ibarlucea-Benitez, I., Muller, D. J., Paluch, E. and Heisenberg, C. P. (2010). Control of directed cell migration in vivo by membrane-to-cortex attachment. *PLoS Biol.* **8**, e1000544.
Dong, M., Fu, Y. F., Du, T. T., Jing, C. B., Fu, C. T., Chen, Y., Jin, Y., Deng, M. and Liu, T. X. (2009). Heritable and lineage-specific gene knockdown in zebrafish embryo. *PLoS ONE* **4**, e6125.
Drees, F., Pokutta, S., Yamada, S., Nelson, W. J. and Weis, W. I. (2005). Alpha-catenin is a molecular switch that binds E-cadherin-beta-catenin and regulates actin-filament assembly. *Cell* **123**, 903-915.
Fackler, O. T. and Grosse, R. (2008). Cell motility through plasma membrane blebbing. *J. Cell Biol.* **181**, 879-884.
Fukazawa, C., Santiago, C., Park, K. M., Deery, W. J., Gomez de la Torre Canny, S., Holterhoff, C. K. and Wagner, D. S. (2010). poky/chuk/ikk1 is required for differentiation of the zebrafish embryonic epidermis. *Dev. Biol.* **346**, 272-283.
Gladden, A. B., Hebert, A. M., Schneeberger, E. E. and McClatchey, A. I. (2010). The NF2 tumor suppressor, Merlin, regulates epidermal development through the establishment of a junctional polarity complex. *Dev. Cell* **19**, 727-739.
Halbleib, J. M. and Nelson, W. J. (2006). Cadherins in development: cell adhesion, sorting, and tissue morphogenesis. *Genes Dev.* **20**, 3199-3214.
Hammerschmidt, M. and Wedlich, D. (2008). Regulated adhesion as a driving force of gastrulation movements. *Development* **135**, 3625-3641.
Harris, T. J. and Tepass, U. (2010). Adherens junctions: from molecules to morphogenesis. *Nat. Rev. Mol. Cell Biol.* **11**, 502-514.
Kane, D. A., McFarland, K. N. and Warga, R. M. (2005). Mutations in half baked/E-cadherin block cell behaviors that are necessary for teleost epiboly. *Development* **132**, 1105-1116.
Kardash, E., Reichman-Fried, M., Maitre, J. L., Boldajipour, B., Papusheva, E., Messerschmidt, E. M., Heisenberg, C. P. and Raz, E. (2010). A role for Rho GTPases and cell-cell adhesion in single-cell motility in vivo. *Nat. Cell Biol.* **12**, 47-53.
Kimmel, C. B., Ballard, W. W., Kimmel, S. R., Ullmann, B. and Schilling, T. F. (1995). Stages of embryonic development of the zebrafish. *Dev. Dyn.* **203**, 253-310.
Kitt, K. N. and Nelson, W. J. (2011). Rapid suppression of activated Rac1 by cadherins and nectins during de novo cell-cell adhesion. *PLoS ONE* **6**, e17841.
Kofron, M., Spagnuolo, A., Klymkowsky, M., Wylie, C. and Heasman, J. (1997). The roles of maternal alpha-catenin and plakoglobin in the early Xenopus embryo. *Development* **124**, 1553-1560.
Koppen, M., Fernandez, B. G., Carvalho, L., Jacinto, A. and Heisenberg, C. P. (2006). Coordinated cell-shape changes control epithelial movement in zebrafish and Drosophila. *Development* **133**, 2671-2681.
Kovacs, M., Toth, J., Hetenyi, C., Malnasi-Csizmadia, A. and Sellers, J. R. (2004). Mechanism of blebbistatin inhibition of myosin II. *J. Biol. Chem.* **279**, 35557-35563.
Krauss, S., Maden, M., Holder, N. and Wilson, S. W. (1992). Zebrafish pax[b] is involved in the formation of the midbrain-hindbrain boundary. *Nature* **360**, 87-89.
Lepage, S. E. and Bruce, A. E. E. (2010). Zebrafish epiboly: mechanics and mechanisms. *Int. J. Dev. Biol.* **54**, 1213-1228.
Lin, F., Chen, S., Sepich, D. S., Panizzi, J. R., Clendenon, S. G., Marrs, J. A., Hamm, H. E. and Solnica-Krezel, L. (2009). Galpha12/13 regulate epiboly by inhibiting E-cadherin activity and modulating the actin cytoskeleton. *J. Cell Biol.* **184**, 909-921.
Link, V., Carvalho, L., Castanon, I., Stockinger, P., Shevchenko, A. and Heisenberg, C. P. (2006). Identification of regulators of germ layer morphogenesis using proteomics in zebrafish. *J. Cell Sci.* **119**, 2073-2083.
Pilot, F., Philippe, J. M., Lemmers, C. and Lecuit, T. (2006). Spatial control of actin organization at adherens junctions by a synaptotagmin-like protein Btsz. *Nature* **442**, 580-584.
Rimm, D. L., Koslov, E. R., Kebriaei, P., Cianci, C. D. and Morrow, J. S. (1995). Alpha 1(E)-catenin is an actin-binding and -bundling protein mediating the attachment of F-actin to the membrane adhesion complex. *Proc. Natl. Acad. Sci. USA* **92**, 8813-8817.
Saude, L., Woolley, K., Martin, P., Driever, W. and Stemple, D. L. (2000). Axis-inducing activities and cell fates of the zebrafish organizer. *Development* **127**, 3407-3417.
Schlegelmilch, K., Mohseni, M., Kirak, O., Pruszak, J., Rodriguez, J. R., Zhou, D., Kreger, B. T., Vasioukhin, V., Avruch, J., Brummelkamp, T. R. et al. (2011). Yap1 acts downstream of alpha-catenin to control epidermal proliferation. *Cell* **144**, 782-795.
Schulte-Merker, S., Ho, R. K., Herrmann, B. G. and Nusslein-Volhard, C. (1992). The protein product of the zebrafish homologue of the mouse T gene is expressed in nuclei of the germ ring and the notochord of the early embryo. *Development* **116**, 1021-1032.
Shapiro, L. and Weis, W. I. (2009). Structure and biochemistry of cadherins and catenins. *Cold Spring Harb. Perspect. Biol.* **1**, a003053.
Shimizu, T., Yabe, T., Muraoka, O., Yonemura, S., Aramaki, S., Hatta, K., Bae, Y. K., Nojima, H. and Hibi, M. (2005). E-cadherin is required for gastrulation cell movements in zebrafish. *Mech. Dev.* **122**, 747-763.
Siddiqui, M., Sheikh, H., Tran, C. and Bruce, A. E. E. (2010). The tight junction component Claudin E is required for zebrafish epiboly. *Dev. Dyn.* **239**, 715-722.
Slanchev, K., Carney, T. J., Stemmler, M. P., Koschorz, B., Amsterdam, A., Schwarz, H. and Hammerschmidt, M. (2009). The epithelial cell adhesion molecule EpCAM is required for epithelial morphogenesis and integrity during zebrafish epiboly and skin development. *PLoS Genet.* **5**, e1000563.
Solnica-Krezel, L. (2005). Conserved patterns of cell movements during vertebrate gastrulation. *Curr. Biol.* **15**, R213-R228.
Speirs, C. K., Jernigan, K. K., Kim, S. H., Cha, Y. I., Lin, F., Sepich, D. S., DuBois, R. N., Lee, E. and Solnica-Krezel, L. (2010). Prostaglandin Gbetagamma signaling stimulates gastrulation movements by limiting cell adhesion through Snai1a stabilization. *Development* **137**, 1327-1337.
Stemmler, M. P. (2008). Cadherins in development and cancer. *Mol. Biosyst.* **4**, 835-850.
Thisse, B. and Thisse, C. (1998). High resolution whole-mount in situ hybridization. *Zebrafish Science Monitor* **5**, 8-9.
Thisse, B., Pflumio, S., Fürthauer, M., Loppin, B., Heyer, V., Degrave, A., Woehl, R., Lux, A., Steffan, T., Charbonnier, X. Q. et al. (2001). Expression of the zebrafish genome during embryogenesis (NIH R01 RR15402). ZFIN Direct Data Submission (http://zfin.org).
Tinevez, J. Y., Schulze, U., Salbreux, G., Roensch, J., Joanny, J. F. and Paluch, E. (2009). Role of cortical tension in bleb growth. *Proc. Natl. Acad. Sci. USA* **106**, 18581-18586.
Torres, M., Stoykova, A., Huber, O., Chowdhury, K., Bonaldo, P., Mansouri, A., Butz, S., Kemler, R. and Gruss, P. (1997). An alpha-E-catenin gene trap mutation defines its function in preimplantation development. *Proc. Natl. Acad. Sci. USA* **94**, 901-906.
Van Furden, D., Johnson, K., Segbert, C. and Bossinger, O. (2004). The C. elegans ezrin-radixin-moesin protein ERM-1 is necessary for apical junction remodelling and tubulogenesis in the intestine. *Dev. Biol.* **272**, 262-276.
Wallingford, J. B., Rowning, B. A., Vogeli, K. M., Rothbacher, U., Fraser, S. E. and Harland, R. M. (2000). Dishevelled controls cell polarity during Xenopus gastrulation. *Nature* **405**, 81-85.
Yamada, S., Pokutta, S., Drees, F., Weis, W. I. and Nelson, W. J. (2005). Deconstructing the cadherin-catenin-actin complex. *Cell* **123**, 889-901.
Yonemura, S., Wada, Y., Watanabe, T., Nagafuchi, A. and Shibata, M. (2010). alpha-Catenin as a tension transducer that induces adherens junction development. *Nat. Cell Biol.* **12**, 533-542.

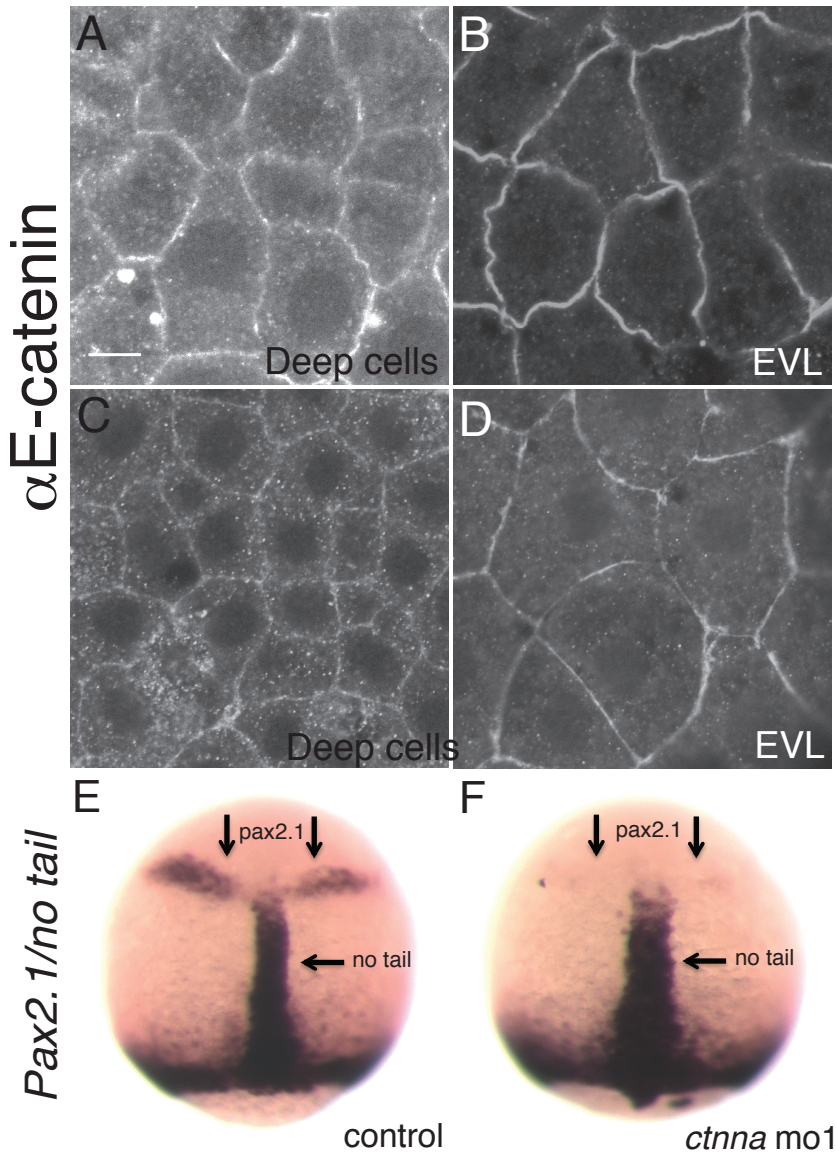
αE-catenin
A
Deep cells
B
EVL
C
Deep cells
D
EVL
Pax2.1/no tail
E
pax2.1
no tail
control
F
pax2.1
no tail
ctnna mo1

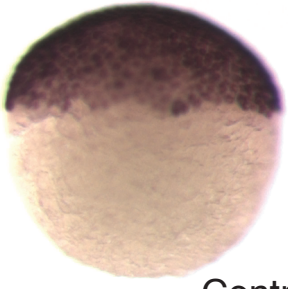

Control

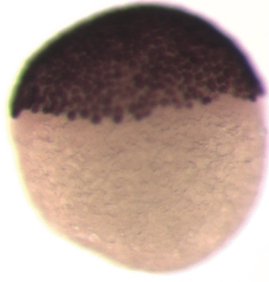

ctnna mo

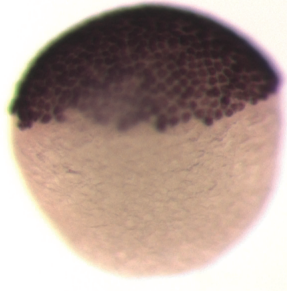

cdh1 mo

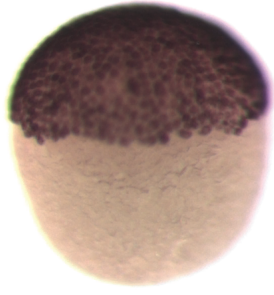

ctnna/cdh1 mo

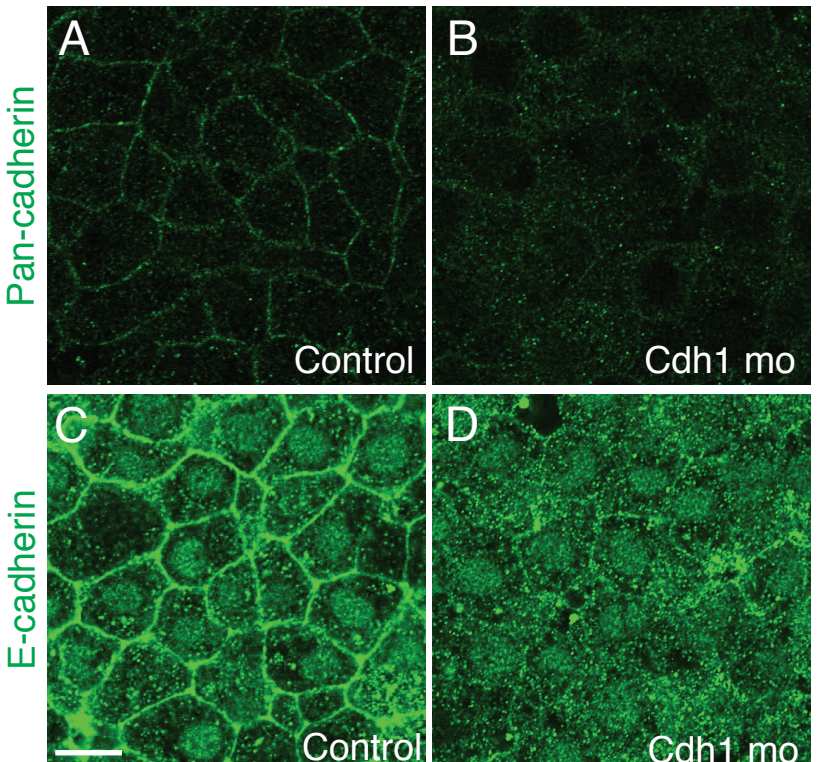
A
B
Pan-cadherin
Control
Cdh1 mo
C
D
E-cadherin
Control
Cdh1 mo

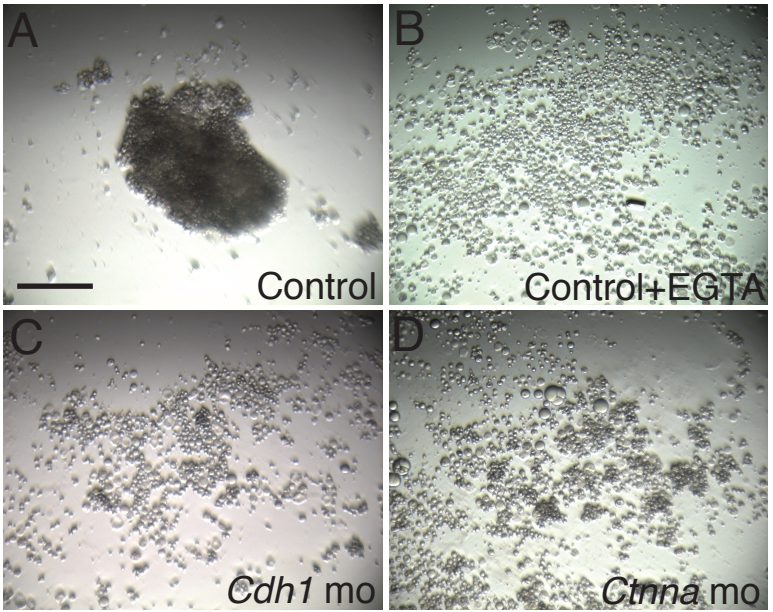
A
Control
B
Control+EGTA
C
Cdh1 mo
D
Ctnna mo

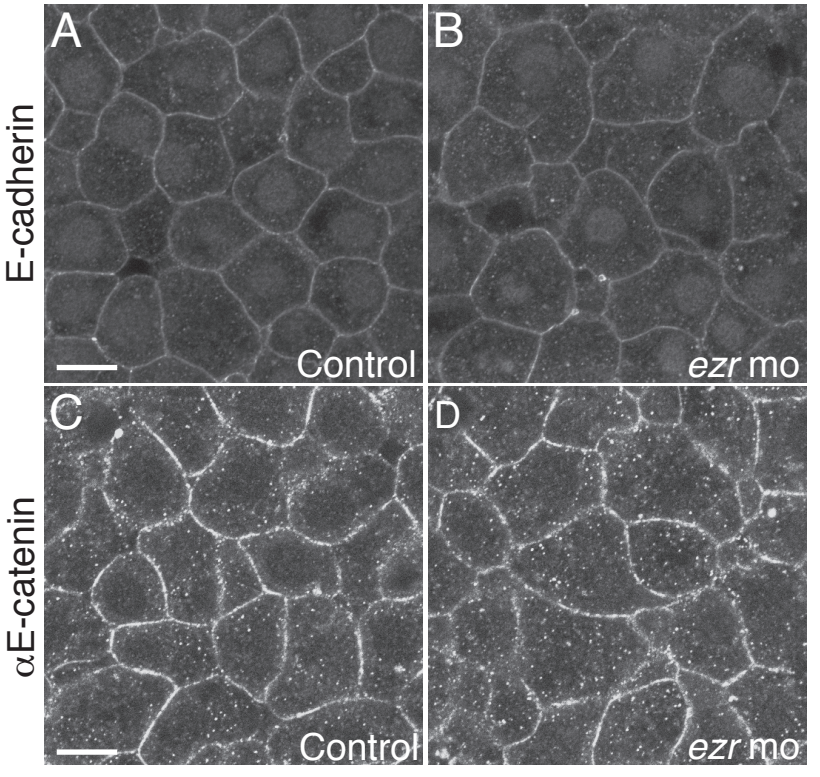
A
B
E-cadherin
Control
ezr mo
C
D
αE-catenin
Control
ezr mo